2017

On the role of the corpus callosum in interhemispheric functional connectivity in humans

Jarod L. Roland
Washington University School of Medicine in St. Louis

Abraham Z. Snyder
Washington University School of Medicine in St. Louis

Carl D. Hacker
Washington University School of Medicine in St. Louis

Anish Mitra
Washington University School of Medicine in St. Louis

Joshua S. Shimony
Washington University School of Medicine in St. Louis

See next page for additional authors

On the role of the corpus callosum in interhemispheric functional connectivity in humans

Jarod L. Roland[a,1], Abraham Z. Snyder[b,c], Carl D. Hacker[a,d], Anish Mitra[b], Joshua S. Shimony[b], David D. Limbrick[a], Marcus E. Raichle[b], Matthew D. Smyth[a], and Eric C. Leuthardt[a,d,e,f,g,h]

[a]Department of Neurological Surgery, Washington University in St. Louis, St. Louis, MO 63110; [b]Mallinckrodt Institute Radiology, Washington University in St. Louis, St. Louis, MO 63110; [c]Neurology, Washington University in St. Louis, St. Louis, MO 63110; [d]Biomedical Engineering, Washington University in St. Louis, St. Louis, MO 63110; [e]Neuroscience, Washington University in St. Louis, St. Louis, MO 63110; [f]Mechanical Engineering and Materials Science, Washington University in St. Louis, St. Louis, MO 63110; [g]Center for Innovation in Neuroscience and Technology, Washington University in St. Louis, St. Louis, MO 63110; and [h]Brain Laser Center, Washington University in St. Louis, St. Louis, MO 63110

Edited by Michel Thiebaut de Schotten, Institut du Cerveau et de la Moelle Épinière, Paris, France, and accepted by Editorial Board Member Marlene Behrmann November 7, 2017 (received for review May 10, 2017)

Resting state functional connectivity is defined in terms of temporal correlations between physiologic signals, most commonly studied using functional magnetic resonance imaging. Major features of functional connectivity correspond to structural (axonal) connectivity. However, this relation is not one-to-one. Interhemispheric functional connectivity in relation to the corpus callosum presents a case in point. Specifically, several reports have documented nearly intact interhemispheric functional connectivity in individuals in whom the corpus callosum (the major commissure between the hemispheres) never develops. To investigate this question, we assessed functional connectivity before and after surgical section of the corpus callosum in 22 patients with medically refractory epilepsy. Section of the corpus callosum markedly reduced interhemispheric functional connectivity. This effect was more profound in multimodal associative areas in the frontal and parietal lobe than primary regions of sensorimotor and visual function. Moreover, no evidence of recovery was observed in a limited sample in which multiyear, longitudinal follow-up was obtained. Comparison of partial vs. complete callosotomy revealed several effects implying the existence of polysynaptic functional connectivity between remote brain regions. Thus, our results demonstrate that callosal as well as extracallosal anatomical connections play a role in the maintenance of interhemispheric functional connectivity.

corpus callosum | resting state | functional connectivity | structural connectivity | callosotomy

Infra-slow (<0.1 Hz) intrinsic brain activity is temporally correlated within functionally related systems currently known as resting state networks (RSNs) (1, 2). This phenomenon is widely known as functional connectivity (FC). RSNs are conveniently studied in humans using resting state functional magnetic resonance imaging (rs-fMRI). Although rs-fMRI is increasingly being used to map the representation of function in health and disease (3–6), the physiological principles underlying RSNs remain incompletely understood (7). In particular, the extent to which anatomical connectivity accounts for FC is unclear. On the one hand, the broad topographic features of RSNs correspond to major white matter tracts. For example, the cingulum bundle connects the anterior and posterior midline components (nodes) of the default mode network (DMN) (8). However, FC generally is more extensive than anatomical connectivity. For example, interhemispheric anatomical connections between the primary visual cortices (V1) in each hemisphere are sparse; yet, V1 homotopic FC is strong (9). Thus, the relation between anatomical and FC remains a topic of active investigation (for a recent review, see ref. 10).

One of the most striking features of resting state FC is symmetry about the midline. Thus, resting state correlations tend to be particularly strong between corresponding loci in each hemisphere (homotopic FC) (11, 12). The corpus callosum (CC) is the major commissure connecting the two hemispheres. Accordingly, it would be logical to suppose that the CC accounts for the prominent symmetry of FC. However, data pertaining to this question are mixed and partially contradictory. One set of pertinent observations derives from human studies of callosal agenesis, a condition in which the CC never develops. An early study reported that homotopic FC is decreased but not absent (13). More recent papers emphasize that homotopic FC in callosal agenesis may be nearly normal (14–17). Conflicting inferences might be drawn from observations made in patients with intractable epilepsy who have undergone therapeutic section of the CC (18–20). Specifically, Johnston et al. studied a 6-y-old boy before and after a complete callosotomy and reported that FC was normal before surgery but largely lost afterward (18). However, Uddin et al. found partially intact interhemispheric FC four decades after total callosotomy (20). A recent study in monkeys observed marked loss of homotopic FC following complete section of the CC, but only in cases in which the anterior commissure also was sectioned (21). Division of the anterior commissure along with corpus callosotomy varied among the three reports mentioned above. Specifically, the anterior commissure was spared in the case reported by Johnston et al., sectioned in the case reported by Uddin et al., and sectioned in

Significance

The relation between structural and functional connectivity has profound implications for our understanding of cerebral physiology and cognitive neuroscience. Yet, this relation remains incompletely understood. Cases in which the corpus callosum is sectioned for medical reasons provide a unique opportunity to study this question. We report functional connectivity assessed before and after surgical section of the corpus callosum, including multiyear follow-up in a limited subsample. Our results demonstrate a causal role for the corpus callosum in maintaining functional connectivity between the hemispheres. Additionally, comparison of results obtained in complete vs. partial callosotomy demonstrate that polysynaptic connections also play a role in maintaining interhemispheric functional connectivity.

Author contributions: J.L.R., J.S.S., D.D.L., M.E.R., M.D.S., and E.C.L. designed research; J.L.R., A.Z.S., A.M., D.D.L., and M.D.S. performed research; J.L.R., A.Z.S., C.D.H., D.D.L., and M.D.S. contributed new reagents/analytic tools; J.L.R., A.Z.S., C.D.H., A.M., and E.C.L. analyzed data; and J.L.R., A.Z.S., and E.C.L. wrote the paper.

Conflict of interest statement: E.C.L. discloses financial relationships with the following companies: Intellectual Ventures, Monteris Medical, Acera Medical, Pear Therapeutics, General Sensing, Immunovalent, Face to Face Biometrics, Neurolutions, and Osteovantage.

This article is a PNAS Direct Submission. M.T.d.S. is a guest editor invited by the Editorial Board.

[1]To whom correspondence should be addressed. Email: rolandj@wustl.edu.

This article contains supporting information online at www.pnas.org/lookup/suppl/doi:10.1073/pnas.1707050114/-/DCSupplemental.

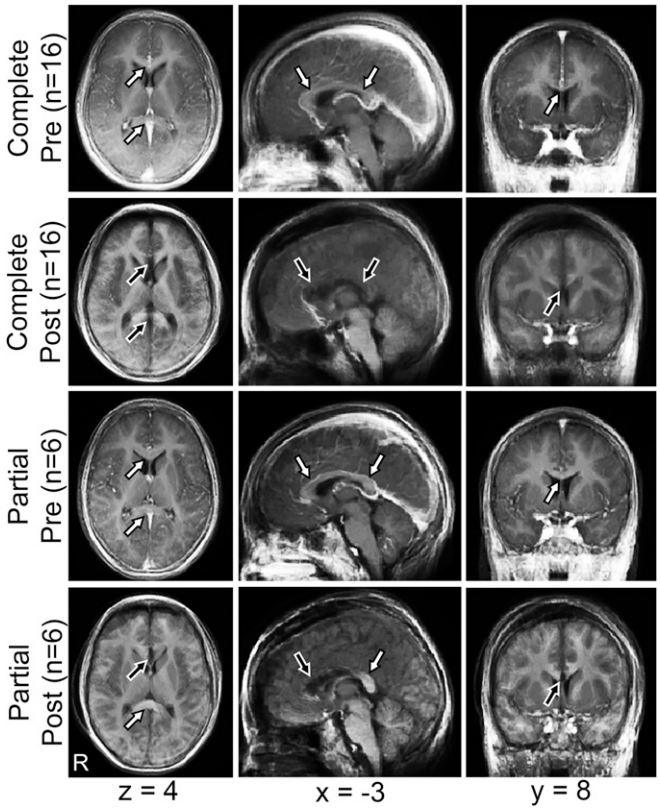

Fig. 1. Anatomic imaging precallosotomy and postcallosotomy. Mean T1-weighted images before (precallosotomy) and after (postcallosotomy) complete and partial callosotomy, represented in atlas space (right hemisphere on *Left*). MNI152 coordinates of axial, sagittal, and coronal planes are listed. White arrows indicate intact CC, and black arrows indicate areas of divided CC. Note residual splenium after partial callosotomy.

two of the three monkeys studied by O'Reilly (21). Thus, the available data do not clearly define the role of the CC in the maintenance of FC.

We acquired rs-fMRI before and after corpus callosotomy in 22 epilepsy patients. The study cohort included partial as well as complete section of the CC, thereby enabling examination of graded effects of callosotomy. Importantly, we also studied select individuals 2–7 y following callosotomy. Our analysis reveals differential contributions of the CC to FC evaluated in different regions of the brain. Specifically, interhemispheric FC in primary sensorimotor and primary visual cortex is less dependent on the CC than multimodal cortex. Interhemispheric FC is decreased immediately after callosotomy and does not show signs of recovery on multiyear longitudinal follow-up.

Results

Structural Imaging. Atlas transformed anatomic images, averaged across subjects, precallosotomy and postcallosotomy, are shown in Fig. 1. White arrows identify normal CC. Black arrows indicate areas where the CC has been sectioned. Spared fibers in the splenium of the CC are evident in the postpartial callosotomy group (white arrows). A voxel-based analysis of the CC area spared by partial callosotomy is shown in Fig. S1.

FC Maps. FC maps obtained with seeds in primary motor and visual areas, precallosotomy and postcallosotomy, are displayed in Fig. 2. The seed coordinates in MNI152 space were (−40, −23, 53) and (41, −22, 48) for left and right motor and (−8, −83, 0) and (7, −83, 0) for left and right vision, respectively. An exemplar individual is shown in Fig. 2*A*. Group-averaged results representing complete and partial callosotomy are shown in Fig. 2 *B* and *C*, respectively. Precallosotomy FC maps identify the expected sensorimotor (SMN) and visual (VIS) networks. The SMN includes primary motor cortex in the precentral gyrus, primary sensory cortex in the postcentral gyrus, and the supplementary motor area in the posterior aspect of the superior frontal gyrus. VIS areas include primary visual cortex in the calcarine sulcus and secondary visual areas in the lateral occipital lobe.

Complete callosotomy, on average (Fig. 2*B*), resulted in a marked loss of interhemispheric FC and, possibly, modest enhancement of intrahemispheric FC, both for motor and visual seeds. The effects of partial callosotomy were different in somatosensory vs. visual areas. Specifically, interhemispheric FC was lost in SMN areas, much as in complete callosotomy. In contrast, interhemispheric FC in VIS areas was largely unaffected by partial callosotomy (Fig. 2*C*). The contrast between partial vs. complete callosotomy most likely reflects sparing of occipital, but not more anterior, commissural fibers. Thus,

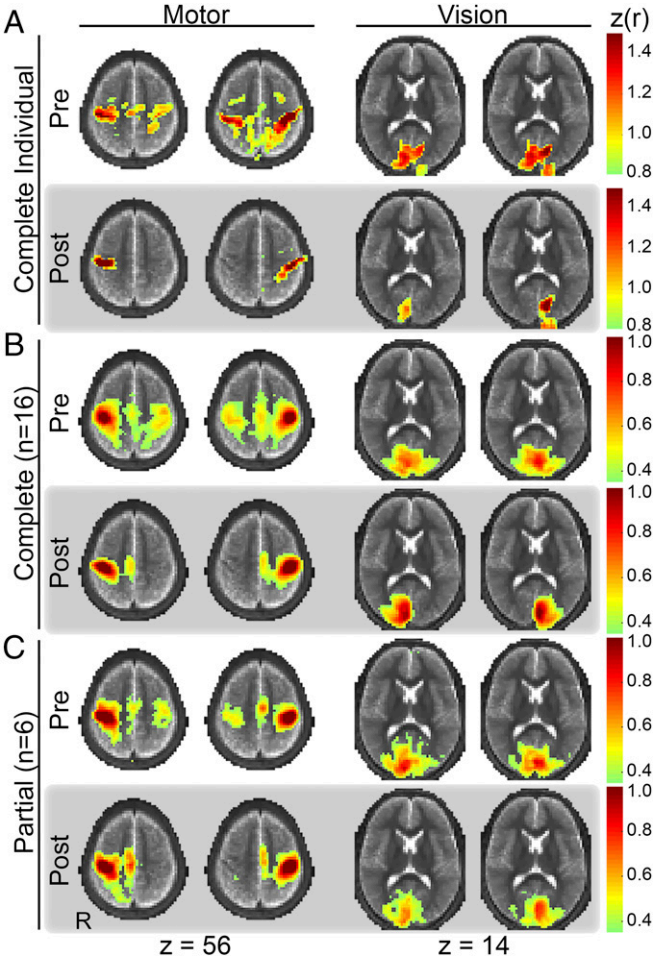

Fig. 2. FC maps corresponding to seeds in primary motor (first and second columns) and primary visual (third and fourth columns) areas of the right (first and third columns) and left (second and fourth columns) hemispheres. (*A*) Results obtained in an exemplar individual. Note loss of interhemispheric FC after complete callosotomy with preserved intrahemispheric FC in both motor and visual networks. (*B*) Mean (n = 16) results before and after complete callosotomy. (*C*) Mean (n = 6) results before and after partial callosotomy. Note maintained visual but not motor interhemispheric FC after partial, but not complete, callosotomy. The FC maps are thresholded at $z(r) >$ 0.80 in the exemplar individual and $z(r) > 0.35$ in the group results.

spared splenial connections between posterior occipital areas continue to mediate interhemispheric FC.

FC Matrices. A previously defined seed set was used for further analysis (3). Seeds in this set were defined by systematic evaluation of previously published literature to best represent seven canonical networks commonly used in resting state fMRI studies. These networks include the dorsal attention network (DAN), ventral attention network (VAN), SMN, VIS, frontal-parietal control network (FPC), language network (LAN), and DMN. Seeds close to the midline (n = 29) were removed from the original set (n = 169). In Fig. 3*C*, the remaining seeds (n = 140) are color coded by RSN.

FC between all seed pairs, sorted by hemisphere and by RSN, is shown in matrix form in Fig. 3*A*. This seed ordering arranges left and right intrahemispheric FC in the top-left and bottom-right quadrants, respectively. The top-right quadrant shows interhemispheric FC. Percent difference was calculated in each individual as $\%\Delta_z = 100 \times (z(r)_{post} - z(r)_{pre})/\max(z(r)_{pre})$, where $z(r)$ is the Fisher z-transformed Pearson correlation coefficient. The $\%\Delta_z$ values shown in Fig. 3*A* are averaged over individuals. A striking decrease in interhemispheric FC is evident after complete callosotomy. Partial callosotomy decreased interhemispheric correlations to a lesser degree. The greatest residual interhemispheric FC was observed between seeds in the visual network. Of note, partial and complete callosotomy similarly decreased FC in the sensorimotor network. We also observed an increase in intrahemispheric FC after both complete and partial callosotomy, which is evident in the difference matrices of Fig. 3*A*. This finding may be related to similar functional imaging results in stroke studies where intrahemispheric FC is found to increase within the hemisphere contralateral to the lesion (22, 23).

To quantify the change in FC after callosotomy, we computed the similarity (element-wise Pearson correlation) between pre- and post-FC matrices. This analysis was partitioned by interhemispheric and intrahemispheric FC. The precallosotomy FC matrices were similar between complete and partial groups with a correlation of r = 0.79. We expected intrahemispheric FC to be affected less by callosotomy and, therefore, served as a control for the changes in interhemispheric FC. Accordingly, the similarity of intrahemispheric FC matrices was not significantly different between right and left hemispheres for either complete {t (30) = 0.505, confidence interval (CI) of difference = [−0.081, 0.134], P = 0.618} or partial {t (30) = 0.054, CI = [−0.158, 0.166], P = 0.958} callosotomy ("Intra" bars in Fig. 3*B*). In contrast, interhemispheric FC was markedly reduced following callosotomy after both complete {t (30) = −7.863, CI = [−0.418, −0.246], P < 0.001 for inter- vs. intraright; and t (30) = −6.797, CI = [−0.397, −0.214], P = <0.001 for inter- vs. intraleft} and partial {t (10) = −2.427, CI = [−0.420, −0.018], P = 0.036 for inter- vs. intraright; and t (10) = −2.267, CI = [−0.426, −0.007], P = 0.047 for inter- vs. intraleft} callosotomy ("Inter" bars in Fig. 3*B*).

Voxel Mirrored Homotopic FC. The present data inform the question of how much FC is or is not attributable to anatomic connectivity. Thus, if homotopic FC were entirely mediated by the CC, then this measure should be eliminated by complete callosotomy. Similarly, partial callosotomy should demonstrate a topographic distinction between preserved vs. eliminated homotopic FC in close relation to the extent of callosotomy. As illustrated in Fig. 4, these predictions are only partially supported

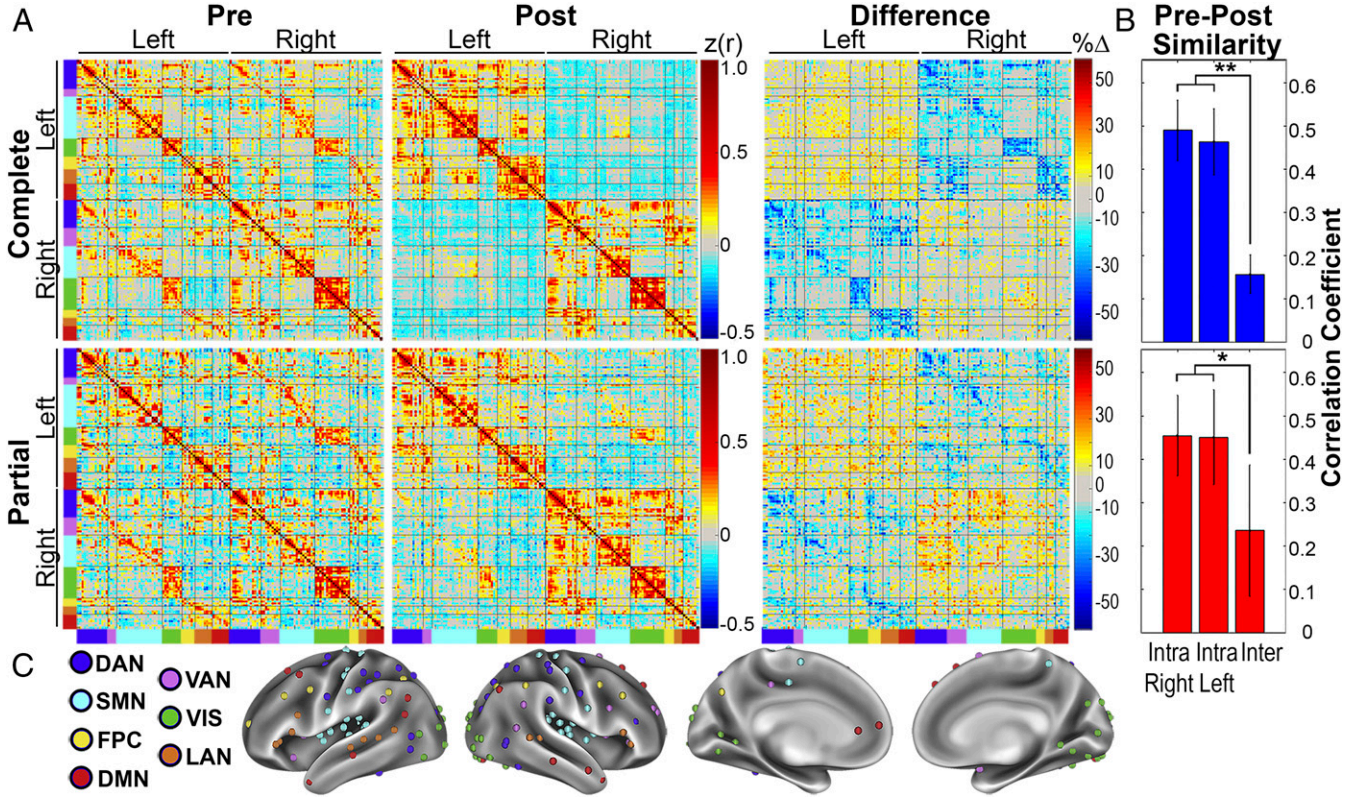

Fig. 3. Contrast between interhemispheric vs. intrahemispheric FC. (*A*) FC matrices representing seven RSNs are organized according to hemisphere of seed. Diagonal and off-diagonal blocks represent intrahemispheric and interhemispheric FC, respectively. RSN color codes are defined in *C*. (*B*) Bar graphs representing similarity between precallosotomy and postcallosotomy for intrahemispheric and interhemispheric FC. The error bars represent 95% confidence intervals. $^{**}P < 0.001$, $^{*}P < 0.05$. (*C*) Seeds plotted on an inflated mean brain surface.

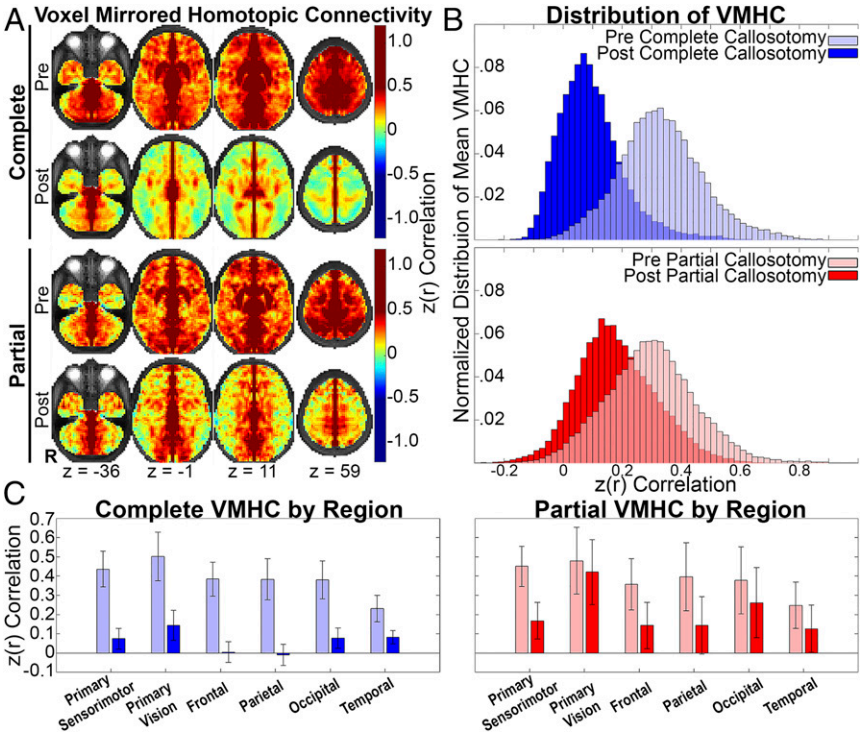

Fig. 4. Topography of CC-mediated FC and distribution of VMHC. (*A*) VMHC computed as the Fisher z-transformed Pearson correlation between voxels mirrored about the midline. By definition, these displays are bilaterally symmetric. Spatial blurring during preprocessing generates artifactually high homotopic FC along the midline. The underlay is the T2-weighted atlas representative image. (*B*) Distributions of mean VMHC across all voxels after vs. before callosotomy. Note larger shift toward zero after complete relative to partial callosotomy. (*C*) Bar graphs (mean ± 95% confidence interval) representing homotopic FC organized according to anatomical region. Note partial preservation of FC in primary sensorimotor and visual cortices after complete callosotomy but nearly complete loss of VMHC in multimodal associative areas. Note also more retained VMHC after partial callosotomy.

by the data. Specifically, as predicted, homotopic FC is markedly reduced in many parts of the brain following complete callosotomy. Similarly, homotopic FC is almost intact in visual areas following partial callosotomy, which spares the splenium, that is, the interhemispheric connection between the occipital lobes. However, homotopic FC is partially preserved in primary sensorimotor and visual areas following complete callosotomy. Similarly, following partial callosotomy, homotopic FC is reduced but not eliminated in many parts of the cerebral hemispheres that, theoretically, have been disconnected. Complete maps for each group before and after are presented in Fig. S3.

To obtain a quantitative view of the contrasting effects of complete vs. partial callosotomy, the distribution of voxel mirrored homotopic FC (VMHC) between all voxels was averaged across individuals. These results are displayed in histogram format in Fig. 4*B*. At baseline (precallosotomy), the distribution of VMHC is similar between complete and partial groups (Cohen's $d = 0.23$). The postcallosotomy distributions clearly are shifted toward zero (i.e., no homotopic FC). However, this effect is much more marked in the complete as opposed to partial callosotomy results (Cohen's d between precallosotomy and postcallosotomy is 0.80 for partial and 1.80 for complete). Positive skew, evident in the postcomplete callosotomy histogram, most likely reflects focal areas of preserved homotopic FC.

To quantify the regional specificity in CC-mediated FC, we evaluated the mean VMHC in primary and multimodal regions before and after callosotomy (Fig. 4*C*). These regions were defined by Brodmann areas corresponding to primary sensorimotor cortex, primary visual cortex, and multimodal areas of frontal, parietal, occipital, and temporal lobes (Fig. S4). The results of this anatomic region of interest analysis are consistent with a more significant decrease in all regions after complete compared with partial callosotomy (*SI Results*). More specifically, after complete callosotomy, multimodal areas of the frontal and parietal lobes are reduced to near zero VMHC, while primary sensorimotor and vision areas are reduced but not lost. In contrast, after partial callosotomy, the primary visual cortex remains near precallosotomy levels, likely owing to the spared splenium fibers.

Follow-Up Imaging at Delayed Time Interval. The postcallosotomy results shown so far demonstrate a marked loss of interhemispheric FC following callosotomy. However, these data were obtained 1 d after surgery, whereas previously reported, albeit limited, evidence raises the possibility that interhemispheric FC may recover after a prolonged interval following complete callosotomy (20). We were able to examine this question in three individuals at intervals between 2 and 7 y after callosotomy (Fig. 5) (*SI Results*). All show no evidence of recovered interhemispheric FC.

Discussion

The extent to which interhemispheric FC depends on the CC is uncertain owing to conflicting evidence. To address this issue, we report a series of human subjects studied before and after surgical section of an intact CC. Our data reveal a causal role of the CC in maintaining interhemispheric FC throughout the brain. Complete section of the CC dramatically reduced interhemispheric FC assessed in the immediate postoperative period, as previously reported in one case study (18). The effects of partial callosotomy were less dramatic and not entirely consistent with a simple relation between structural and FC. We also obtained longitudinal rs-fMRI in a restricted sample of individuals studied between 2 and 7 y following callosotomy. This data speaks to the question of FC plasticity. In the following discussion, we address the relation between structural and FC. We also touch on the question of interhemispheric FC recovery following a prolonged postoperative interval.

Structural Versus FC. Previous studies report a correlation between cortical areas with strong structural and FC, but this relationship is incomplete in other areas with strong FC but weak structural connectivity (8, 24, 25). These findings imply that the relation between structural and FC is not one-to-one. Nevertheless, the most salient characteristics of resting state is strong homotopic FC (11), and the largest white matter structure in the brain is the CC. It is therefore reasonable to assume that the CC plays a major role in the maintenance of homotopic FC. Acknowledging expected differences at baseline from typically developing

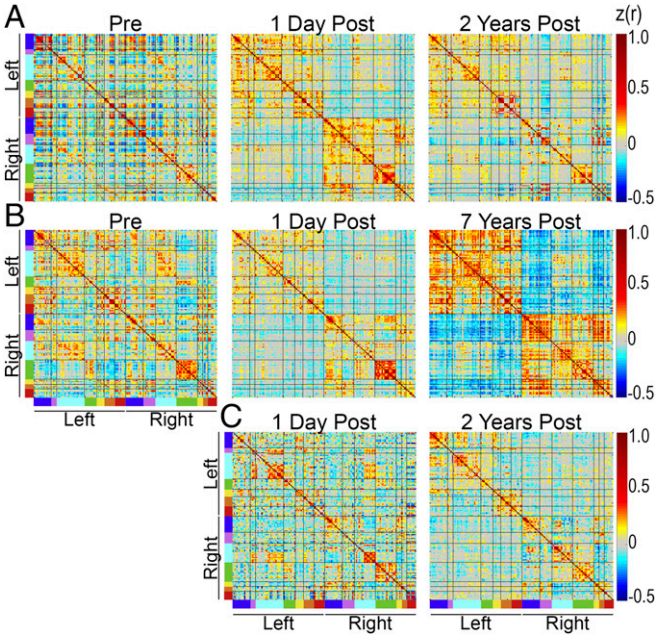

Fig. 5. FC matrices obtained in three individuals including longitudinal imaging at follow-up intervals of 2–7 y. (*A*) Partial callosotomy at age 2 y; follow-up (sedated) at age 4 y. (*B*) Complete callosotomy at age 13 y; follow-up (nonsedated) at age 20 y. (*C*) Complete callosotomy at age 15 y; follow-up (sedated) at age 17 y. The precallosotomy study in this case was excluded as this patient initially presented with epileptic encephalopathy. Follow-up imaging 2 y after complete callosotomy was obtained under sedation for clinical indications. Note no sign of recovery of interhemispheric FC at follow-up in any of these individuals.

individuals, we focus our study on precallosotomy vs. postcallosotomy FC differences within subject.

Our results show partially preserved homotopic FC following complete callosotomy in primary sensorimotor and visual areas (Fig. 4 *A* and *C*). Hence, structures other than the CC must be contributory. Two observations inform this question. First, invasive tracer studies show relatively sparse axonal connectivity via the CC in the hand area of primary motor cortex ("callosal holes") (26–28). Also, it is known that callosal connections between primary visual areas are very sparse (29–31). Thus, it may be inferred that homotopic FC in primary cortical areas is less dependent on the CC. Second, prior studies have established that subcortical structures participate in resting-state cortical RSNs (32, 33). Importantly, the most robust thalamocortical structural connectivity, as assessed by DTI tractography, is found in primary sensorimotor and visual cortices, whereas the weakest connections are found in multimodal areas (34). This anatomy is consistent with the residual FC evident in Fig. 4*A*.

Further evidence of polysynaptic FC is apparent after partial callosotomy (Fig. 4*A*). Homotopic FC in multimodal areas of the frontal lobes is reduced less after partial relative to complete callosotomy, despite callosal fibers connecting these areas sectioned in both procedures. This is in contrast to residual interhemispheric FC in posterior parietal and occipital areas, which is expected from known structural connections in the splenium (35). This finding suggests that posterior parietal-occipital areas, the callosal fibers of which are spared by partial callosotomy, are able to support frontal homotopic FC via intrahemispheric anatomic connections, e.g., via the superior longitudinal fasciculus. Thus, the posterior areas with maintained callosal structural connectivity act as hubs between widely separated regions in posterior and anterior parts of the brain. These findings help to explain the absence of disconnection syndrome after partial callosotomy where interhemispheric information transfer remains when the splenium is spared (36).

Homotopic FC data has been reported in prior studies (11) and summarized by metaanalysis (37). Homotopy is a consistent characteristic of resting-state fMRI (12) with electrophysiological correlates (38). Notable exceptions are language and attention functionality, which are asymmetrically represented in the human brain (39, 40). Stark et al. (11) show greatest homotopic FC in primary sensorimotor areas, followed by unimodal and heteromodal association areas. We observe similar results of greatest residual interhemispheric FC after callosotomy in the sensorimotor and vision networks, as well as near zero VMHC after complete callosotomy in frontal and parietal regions.

Longitudinal Follow-Up. Previously reported postcallosotomy imaging has been obtained at intervals ranging from 1 d (18) to 6 mo (21) to 4 decades (20). The strongest evidence of FC recovery following a prolonged interval was reported in ref. 20. In our cohort, only one individual was able to tolerate nonsedated follow-up imaging. In two other individuals, sedated imaging was obtained for clinical indications. Our follow-up data reveal no convincing evidence of recovery of interhemispheric FC several years after callosotomy. These results tend to validate our postcallosotomy data obtained at an interval of 1 d.

The observation of relatively intact interhemispheric FC in callosal agenesis (e.g., ref. 16) raises the question whether compensation for the absence of a CC is possible very early in development within a critical period. Indeed, diffusion tensor MRI results indicate that compensatory tracts in the anterior and posterior commissures develop in these cases (16). The present follow-up data suggest that such compensation does not occur postnatally even in a case as young as 2 y. Thus, if a critical period does exist, it would seem to be over by age 2 y. Accordingly, it is not surprising that we saw no evidence of recovery in the other two longitudinally studied individuals. Our data, however, do not exclude the possibility of recovery decades following callosotomy (20).

Conclusion

We expand the available data that heretofore has been derived from a very limited number of case studies of corpus callosotomy. In particular, this is the only study to date reporting longitudinal human FC data acquired at an interval of years. We find no evidence of interhemispheric FC recovery. We provide strong evidence supporting a causal role of the CC in maintaining interhemispheric FC. We also provide evidence that extracallosal pathways are important, specifically in mediating residual homotopic FC in primary sensorimotor and visual areas following complete callosotomy. More generally, our results reinforce the principle that polysynaptic pathways account for a substantial fraction of FC (41, 42).

Methods

Corpus Callosotomy Subjects. Twenty-two individuals with medically refractory epilepsy underwent complete (n = 16) or partial (n = 6) corpus callosotomy according to standard practice (43). All aspects of the study were approved by the Human Research and Protection Office Institutional Review Board (IRB) at Washington University School of Medicine in St. Louis. All subjects were pediatric patients with cognitive disabilities, therefore informed consent was initially obtained from the parent or legal guardian with assent from the subject where appropriate. The IRB subsequently approved waiver of written consent for imaging sequences obtained alongside clinical studies. The subjects who returned for delayed follow-up imaging provided an additional informed consent from the parent or legal guardian with assent when appropriate. Surgical candidacy was determined by clinical criteria alone. See *SI Methods* for further details.

Callosotomy Procedure. Corpus callosotomy was performed following a standard clinical protocol via open craniotomy and microsurgical technique, as previously described (43) (*SI Methods*). Complete callosotomy divides the entire length of the CC including the splenium. In partial callosotomy, the posterior third to fourth of the CC (always including the splenium) is spared. Postoperative imaging is routinely obtained 1 d after surgery to confirm planned extent of callosotomy and rule out any surgical complications.

Image Acquisition and Preprocessing. All imaging was performed with a 3T Siemens Trio scanner. Structural imaging included one T1w MP-RAGE [repetition time (TR) = 2,000 ms, echo time (TE) = 2.5 ms, flip angle = 12°, voxel size 1.0 × 1.0 × 1.0 mm] and one T2-weighted (T2w) turbo-spin echo sequence [TR = 9,000 ms, TE = 115 ms, flip angle = 120°, voxel size 1.0 × 1.0 × 2.5 mm]. For clinical reasons, the preoperative (but not postoperative) MP-RAGE was acquired with i.v. gadolinium contrast (at the end of the session). The remaining sequences were identical across sessions. Resting-state fMRI was acquired using an echo-planar imaging (EPI) sequence sensitive to blood oxygen level-dependent (BOLD) contrast (TR = 2,070 ms, TE = 25 ms, flip angle = 90°, voxel size 4.0 × 4.0 × 4.0 mm). Two runs of 200 frames each (~14 min total) were acquired in each subject. Preprocessing followed previously published methods (44) (*SI Methods*).

FC. FC was computed using seed-based correlation analysis with a previously defined seed set (3) (Fig. 3). Each 6-mm spherical seed was assigned to one of seven canonical RSNs. Of the original 169 seeds, 29 near the midline were excluded to reduce overlap from common source location and spatial blurring. FC, defined as the Pearson correlation coefficient (r), was computed between the seed and every other voxel in the brain. Pearson r values were Fisher z-transformed in all subsequent analysis.

ACKNOWLEDGMENTS. We thank Nicholas Szrama, Mrinal Pawa, Ravi Chacko, Joseph Humphries, Donna Dierker, Nicholas Metcalf, and Mario Ortega for useful contributions, discussions, and guidance during data analysis and manuscript preparation, and we thank the patients and their families for contributing to this research. This study was supported by NIH Grant R25 NS090978, the Knight-Davidson family, The McDonnell Center for Systems Neuroscience, Eunice Kennedy Shriver National Institute of Child Health & Human Development of the National Institutes of Health under Award U54 HD087011 to the Intellectual and Developmental Disabilities Research Center at Washington University in St. Louis, and Neuroimaging Informatics and Analysis Center Grant 1P30NS098577.

1. Shen HH (2015) Core concept: Resting-state connectivity. *Proc Natl Acad Sci USA* 112: 14115–14116.
2. Snyder AZ (2016) Intrinsic brain activity and resting state networks. *Neuroscience in the 21st Century*, eds Pfaff DW, Volkow ND (Springer, New York), pp 1–52.
3. Hacker CD, et al. (2013) Resting state network estimation in individual subjects. *Neuroimage* 82:616–633.
4. Leuthardt EC, et al. (2015) Resting-state blood oxygen level-dependent functional MRI: A paradigm shift in preoperative brain mapping. *Stereotact Funct Neurosurg* 93: 427–439.
5. Brier MR, Day GS, Snyder AZ, Tanenbaum AB, Ances BM (2016) N-methyl-D-aspartate receptor encephalitis mediates loss of intrinsic activity measured by functional MRI. *J Neurol* 263:1083–1091.
6. Smyser CD, et al. (2016) Resting-state network complexity and magnitude are reduced in prematurely born infants. *Cereb Cortex* 26:322–333.
7. Schölvinck ML, Leopold DA, Brookes MJ, Khader PH (2013) The contribution of electrophysiology to functional connectivity mapping. *Neuroimage* 80:297–306.
8. Greicius MD, Supekar K, Menon V, Dougherty RF (2009) Resting-state functional connectivity reflects structural connectivity in the default mode network. *Cereb Cortex* 19:72–78.
9. Vincent JL, et al. (2007) Intrinsic functional architecture in the anaesthetized monkey brain. *Nature* 447:83–86.
10. Behrens TE, Sporns O (2012) Human connectomics. *Curr Opin Neurobiol* 22:144–153.
11. Stark DE, et al. (2008) Regional variation in interhemispheric coordination of intrinsic hemodynamic fluctuations. *J Neurosci* 28:13754–13764.
12. Salvador R, et al. (2005) Neurophysiological architecture of functional magnetic resonance images of human brain. *Cereb Cortex* 15:1332–1342.
13. Quigley M, et al. (2003) Role of the corpus callosum in functional connectivity. *AJNR Am J Neuroradiol* 24:208–212.
14. Tyszka JM, Kennedy DP, Adolphs R, Paul LK (2011) Intact bilateral resting-state networks in the absence of the corpus callosum. *J Neurosci* 31:15154–15162.
15. Khanna PC, et al. (2012) Preserved interhemispheric functional connectivity in a case of corpus callosum agenesis. *Neuroradiology* 54:177–179.
16. Tovar-Moll F, et al. (2014) Structural and functional brain rewiring clarifies preserved interhemispheric transfer in humans born without the corpus callosum. *Proc Natl Acad Sci USA* 111:7843–7848.
17. Owen JP, et al. (2013) Resting-state networks and the functional connectome of the human brain in agenesis of the corpus callosum. *Brain Connect* 3:547–562.
18. Johnston JM, et al. (2008) Loss of resting interhemispheric functional connectivity after complete section of the corpus callosum. *J Neurosci* 28:6453–6458.
19. Pizoli CE, et al. (2011) Resting-state activity in development and maintenance of normal brain function. *Proc Natl Acad Sci USA* 108:11638–11643.
20. Uddin LQ, et al. (2008) Residual functional connectivity in the split-brain revealed with resting-state functional MRI. *Neuroreport* 19:703–709.
21. O'Reilly JX, et al. (2013) Causal effect of disconnection lesions on interhemispheric functional connectivity in rhesus monkeys. *Proc Natl Acad Sci USA* 110:13982–13987.
22. van Meer MP, et al. (2010) Recovery of sensorimotor function after experimental stroke correlates with restoration of resting-state interhemispheric functional connectivity. *J Neurosci* 30:3964–3972.
23. Siegel JS, et al. (2016) Disruptions of network connectivity predict impairment in multiple behavioral domains after stroke. *Proc Natl Acad Sci USA* 113:E4367–E4376.
24. Koch MA, Norris DG, Hund-Georgiadis M (2002) An investigation of functional and anatomical connectivity using magnetic resonance imaging. *Neuroimage* 16:241–250.
25. Honey CJ, et al. (2009) Predicting human resting-state functional connectivity from structural connectivity. *Proc Natl Acad Sci USA* 106:2035–2040.
26. Killackey HP, Gould HJ, 3rd, Cusick CG, Pons TP, Kaas JH (1983) The relation of corpus callosum connections to architectonic fields and body surface maps in sensorimotor cortex of new and old world monkeys. *J Comp Neurol* 219:384–419.
27. Pappas CL, Strick PL (1981) Anatomical demonstration of multiple representation in the forelimb region of the cat motor cortex. *J Comp Neurol* 200:491–500.
28. Iwamura Y, Taoka M, Iriki A (2001) Bilateral activity and callosal connections in the somatosensory cortex. *Neuroscientist* 7:419–429.
29. Van Essen DC, Newsome WT, Bixby JL (1982) The pattern of interhemispheric connections and its relationship to extrastriate visual areas in the macaque monkey. *J Neurosci* 2:265–283.
30. Berlucchi G (2014) Visual interhemispheric communication and callosal connections of the occipital lobes. *Cortex* 56:1–13.
31. Saenz M, Fine I (2010) Topographic organization of V1 projections through the corpus callosum in humans. *Neuroimage* 52:1224–1229.
32. Zhang D, Snyder AZ, Shimony JS, Fox MD, Raichle ME (2010) Noninvasive functional and structural connectivity mapping of the human thalamocortical system. *Cereb Cortex* 20:1187–1194.
33. Bell PT, Shine JM (2016) Subcortical contributions to large-scale network communication. *Neurosci Biobehav Rev* 71:313–322.
34. Toulmin H, et al. (2015) Specialization and integration of functional thalamocortical connectivity in the human infant. *Proc Natl Acad Sci USA* 112:6485–6490.
35. Chao YP, et al. (2009) Probabilistic topography of human corpus callosum using cytoarchitectural parcellation and high angular resolution diffusion imaging tractography. *Hum Brain Mapp* 30:3172–3187.
36. Gordon HW, Bogen JE, Sperry RW (1971) Absence of deconnexion syndrome in two patients with partial section of the neocommissures. *Brain* 94:327–336.
37. Toro R, Fox PT, Paus T (2008) Functional coactivation map of the human brain. *Cereb Cortex* 18:2553–2559.
38. Drew PJ, Duyn JH, Golanov E, Kleinfeld D (2008) Finding coherence in spontaneous oscillations. *Nat Neurosci* 11:991–993.
39. Fox MD, Corbetta M, Snyder AZ, Vincent JL, Raichle ME (2006) Spontaneous neuronal activity distinguishes human dorsal and ventral attention systems. *Proc Natl Acad Sci USA* 103:10046–10051.
40. McAvoy M, et al. (2016) Unmasking language lateralization in human brain intrinsic activity. *Cereb Cortex* 26:1733–1746.
41. Adachi Y, et al. (2012) Functional connectivity between anatomically unconnected areas is shaped by collective network-level effects in the macaque cortex. *Cereb Cortex* 22:1586–1592.
42. Damoiseaux JS, Greicius MD (2009) Greater than the sum of its parts: A review of studies combining structural connectivity and resting-state functional connectivity. *Brain Struct Funct* 213:525–533.
43. Jalilian L, et al. (2010) Complete versus anterior two-thirds corpus callosotomy in children: Analysis of outcome. *J Neurosurg Pediatr* 6:257–266.
44. Shulman GL, et al. (2010) Right hemisphere dominance during spatial selective attention and target detection occurs outside the dorsal frontoparietal network. *J Neurosci* 30:3640–3651.
45. Maccotta L, et al. (2013) Impaired and facilitated functional networks in temporal lobe epilepsy. *Neuroimage Clin* 2:862–872.
46. Reyes A, et al. (2016) Resting-state functional MRI distinguishes temporal lobe epilepsy subtypes. *Epilepsia* 57:1475–1484.
47. Luo C, et al. (2011) Altered functional connectivity in default mode network in absence epilepsy: A resting-state fMRI study. *Hum Brain Mapp* 32:438–449.
48. Power JD, Barnes KA, Snyder AZ, Schlaggar BL, Petersen SE (2012) Spurious but systematic correlations in functional connectivity MRI networks arise from subject motion. *Neuroimage* 59:2142–2154.
49. Mhuircheartaigh RN, et al. (2010) Cortical and subcortical connectivity changes during decreasing levels of consciousness in humans: A functional magnetic resonance imaging study using propofol. *J Neurosci* 30:9095–9102.
50. Fox MD, Zhang D, Snyder AZ, Raichle ME (2009) The global signal and observed anticorrelated resting state brain networks. *J Neurophysiol* 101:3270–3283.
51. Buckner RL, et al. (2004) A unified approach for morphometric and functional data analysis in young, old, and demented adults using automated atlas-based head size normalization: Reliability and validation against manual measurement of total intracranial volume. *Neuroimage* 23:724–738.

Supporting Information

Roland et al. 10.1073/pnas.1707050114

SI Results

VMHC. We quantified the changes in VMHC between precallosotomy and postcallosotomy states by anatomically defined regions in the complete and partial groups. Primary sensorimotor: complete – $t(15) = -6.300$, $P < 0.001$; partial – $t(5) = -4.388$, $P = 0.043$. Primary vision: complete – $t(15) = -4.747$, $P < 0.001$; partial – $t(5) = -0.532$, $P = 0.618$. Frontal: complete – $t(15) = -6.445$, $P < 0.001$; partial – $t(5) = -2.736$, $P = 0.041$. Parietal: complete – $t(15) = -5.712$, $P < 0.001$; partial – $t(5) = -2.388$, $P = 0.063$. Occipital: complete – $t(15) = -5.627$, $P < 0.001$; partial – $t(5) = -1.257$, $P = 0.264$. Temporal: complete – $t(15) = -3.365$, $P = 0.004$; partial – $t(5) = -1.251$, $P = 0.266$.

To further quantify the magnitude of changes by complete and partial groups, we calculated the Cohen's d between precallosotomy and postcallosotomy results for each anatomic region by group. Primary sensorimotor: complete 2.40, partial 2.49; primary vision: complete 1.72, partial 0.30; frontal: complete 2.62, partial 1.48; parietal: complete 2.33, partial: 1.35; occipital: complete 1.94, partial 0.57; temporal: complete 1.38, partial 1.88. The difference in Cohen's d between groups for each region informs us on the magnitude of effect by respective callosotomy. Sorting this difference from greatest to least confirms that the primary vision area shows the greatest difference in FC changes between complete and partial callosotomy (1.41), followed by occipital (1.37), frontal (1.14), parietal (0.99), temporal (0.51), and primary sensorimotor (0.08).

Similar analysis was performed by RSN regions of interest (Fig. S5) as defined by an average RSN parcellation map (Fig. S6). These results demonstrate the frontal and parietal regions observed the greatest reduction in VMHC after complete callosotomy, and the primary vision region was most preserved after partial callosotomy. We measured VMHC in seeds placed in select locations including brain regions not directly connected by CC fibers (Fig. S7). Seeds in the frontal, temporal, and parietal areas exemplify areas disconnected by complete callosotomy. However, the sensorimotor and primary vision areas show VMHC decreases similar to the cerebellum and putamen, areas not expected to be disconnected by callosotomy. The thalamus showed the least decrease in VMHC after complete callosotomy. The seed coordinates in MNI-152 space are as follows: frontal –75, 79, –63; temporal –85, 50, –66; parietal –76, 40, –45; sensorimotor –72, 49, –45; primary vision –69, 26, –64; cerebellum –75, 39, –76; putamen –71, 63, –66; thalamus –69, 53, –61.

Follow-Up Imaging at Delayed Time Interval. The first individual (Fig. 5*A*) underwent partial callosotomy at age 2 y (subject 1, Table S1). Repeat imaging was performed 2 y later. The delayed (2-y postcallosotomy) study showed FC largely similar to the results obtained 1 d after the initial procedure.

The second individual (Fig. 5*B*) underwent complete callosotomy at age 13 y (subject 19, Table S1). Repeat imaging was performed 7 y later. The delayed study showed an unusually large shared variance, as observed in the greater magnitude correlations widely seen in the delayed FC matrix. This feature most likely reflects that this subject uniquely was able to tolerate nonsedated MRI, hence, was studied while awake.

The third individual (Fig. 5*C*) had an acute worsening of seizure frequency at age 15 y, leading to a state of epileptic encephalopathy treated by complete callosotomy. The 1-d postoperative study revealed a markedly disorganized pattern similar to that previously reported in another case of epileptic encephalopathy (19). Repeat imaging, performed 2 y later, showed improved intrahemispheric organization (in association with dramatic improvement in seizure control) but very little interhemispheric FC. Due to acute presentation with epileptic encephalopathy before intervention, preoperative data were not reported and this subject was not included in any of the above group analysis. Propofol was used for sedation at the 1-d and 2-y postcallosotomy time points.

We computed the elementwise correlation coefficient between the precallosotomy, postcallosotomy, and delayed follow-up FC matrices to quantify the change between each time point. These correlations demonstrate a greater similarly between intrahemispheric FC between each time point compared with a least similarity for interhemispheric FC between precallosotomy and immediate postcallosotomy for each subject (Fig. 5*A* – Pre vs. Post: Right 0.40, Left 0.35, Inter 0.05; Post vs. Delay: Right 0.57, Left 0.53, Inter 0.23; Fig. 5*B* – Pre vs. Post: Right 0.57, Left 0.43, Inter 0.23; Post vs. Delay: Right 0.47, Left 0.54, Inter 0.35; Fig. 5*C* – Post vs. Delayed: Right 0.23, Left 0.19, Inter 0.08).

SI Discussion

Patients undergoing corpus callosotomy all have severe, medically refractory epilepsy with nonfocal onset, typically involving drop attacks. These individuals often have significant cognitive deficits. As the profile of pediatric epilepsy is very broad, there is significant variability in medication usage, seizure semiology, and cognitive function. For this reason, we do not attempt to compare the organization of FC to typically developing individuals. Instead, we compare postcallosotomy to precallosotomy FC within individual. Hence, we caution that the results obtained any particular individual in this cohort may be atypical.

Corpus callosotomy is better tolerated at a young age. Therefore, we are unable to study human adults both before and after callosotomy. The individuals in our study were 2–18 y old, which age range spans a significant portion of the postnatal developmental period. Therefore, we expect that our inferences regarding structure-function relations apply generally.

All individuals contributing to the present results were free of gross anatomic lesions on diagnostic imaging. However, the existence of a severe seizure disorder implies that some pathology must be present, notwithstanding no imaging correlate. Emerging evidence has identified various FC abnormalities in different forms of epilepsy (45–47). However, these abnormalities are subtle and, therefore, are unlikely to compromise the present main inferences.

Individuals who are candidates for corpus callosotomy often cannot hold still in a MRI scanner owing to cognitive disability, either as a consequence of long-term epilepsy or comorbid pathology. These individuals cannot be scanned without sedation. Sedation clearly reduces head motion artifact, which otherwise would preclude useful rs-fMRI (48). Fortunately, RSNs are robust to propofol sedation, which is commonly used in ambulatory studies (49). Our study used similar sedation before and after callosotomy (Table S1). However, the requirement for sedation presents an obstacle to clinically not indicated MRI, as sedation is not entirely without risk. This circumstance at least partially accounts for the sparse representation of delayed follow-up rs-fMRI data (ultimately obtained in only 3 of 16 patients).

Apart from the challenges of acquiring rs-fMRI in the callosotomy population, the clinical imaging protocol under which the data were acquired necessitated modifying our approach to image registration. Specifically, precallosotomy T1w scanning was performed with gadolinium contrast, which interferes with

image registration to a conventional T1-weighted atlas template. Hence, atlas registration of the functional data was computed using a newly created T2-weighted template (Fig. S2). Despite these technical difficulties, our methodology produced good image alignment across subjects before and after callosotomy (Fig. 1).

SI Methods

Corpus Callosotomy Subjects. Inclusion criteria included medically refractory epilepsy and no identifiable lesion or structural abnormality (e.g., arachnoid cyst, cortical dysplasia). Patients presenting with acute epileptic encephalopathy requiring urgent intervention were not studied (see Table S1 for demographics). The decision to perform complete or partial callosotomy was decided on the basis of clinical criteria alone by an interdisciplinary epilepsy team consisting of neurosurgeons, neurologists, neuroradiologists, and clinical psychologists. Partial callosotomy is preferred in higher functioning individuals in whom the risk of disconnection syndrome is thought to be high. However, the decision generally is balanced by the consideration that better seizure control is achieved with complete callosotomy (43).

We attempted to contact all subjects for follow-up imaging following the initial postoperative recovery period. This agenda is complicated because many callosotomy patients cannot tolerate nonsedated MRI, whereas the risk of sedation for nonclinically indicated imaging is not easily justified. Therefore, the present study includes only three individuals who returned for follow-up, one of whom was scanned while awake (Fig. 5*B*). One follow-up scan was aborted when the patient refused to enter the MRI.

Callosotomy Procedure. Corpus callosotomy was performed following a standard clinical protocol via open craniotomy and microsurgical technique, as previously described (43). In brief, the head is rigidly fixed in place and frameless stereotactic image guidance is used for neuronavigation. Access is achieved with a coronal or "trap-door" incision and a parasagittal craniotomy eccentric to the right. The craniotomy flap extends ∼4 cm in front of and 2 cm behind the coronal suture and is 4 cm wide. An interhemispheric approach is taken in the plane between the falx and right cerebral hemisphere. An operative microscope is used to enter the avascular midline between the pericallosal arteries. Section of the CC proceeds through a combination of aspiration and bipolar electrocautery.

Image Before and After Processing. Resting-state preprocessing followed standard methodology as has been previously published (44). In brief, this included correction for asynchronous slice acquisition, normalized slice intensity to mode 1,000, and correction of interframe head motion. BOLD data were resampled to 3-mm cubic voxels before time-series correlation analysis. We temporally low-pass filtered the BOLD time series at <0.1 Hz and spatially smoothed it with a 6-mm full-width half-max Gaussian kernel. Nuisance variables included parameters derived from rigid body head motion correction, bilateral lateral ventricle, and white-matter regions of noninterest. The global signal was not included to eliminate any ambiguity in the interpretation of observed findings (50). Following nuisance regression, frame censoring was computed using the temporal derivative of root-mean-square frame-to-frame BOLD signal change across voxels (DVARS). Frames exceeding DVARS = 0.5% were excluded from the FC analyses (48). The DVARS values representing artifact timeseries are plotted in Fig. S8 to demonstrate the very little motion present in our sedated subjects.

The CC was manually traced in the midsagittal using the precallosotomy and postcallosotomy T1w structural images for individuals that underwent partial callosotomy. The ratio of CC area remaining postcallosotomy to precallosotomy was calculated. The similarity of interhemispheric FC between precallosotomy and postcallosotomy was calculated as described in *FC Matrices*. There was not a significant relationship between callosotomy ratio and prepost interhemispheric FC (Pearson correlation $r = 0.52$, $P = 0.29$). This suggests the little variance observed in structural disconnection among patients undergoing partial callosotomy did not correlate with the difference in FC.

In fMRI generally, atlas registration of the functional data are achieved by composition of transforms connecting the EPI, T2w, and T1w images. Conventionally, the T1w structural image is registered to a T1w atlas-representative template. We did not use the preoperative T1w image for atlas registration because it included gadolinium contrast. The postoperative T1w images were also not used for atlas registration because the introduced anatomical deformations, albeit minor, theoretically could have compromised the results. To overcome these barriers, atlas registration was computed via T2w atlas-representative template generated using a previously published strategy (51). Thus, the preoperative T2w (12-parameter affine) was registered to this template. The remaining images then were registered to the preoperative T2w, both within and across sessions (Fig. S2).

We used Matlab 2015b for further data analysis. For statistical tests of precallosotomy and postcallosotomy measures within subject we used paired *t* tests, and for comparison between complete and partial or intrahemispheric and interhemispheric measures, we used the two-sample *t* test. All tests were two-tailed and used a predefined significance threshold of $\alpha = 0.05$.

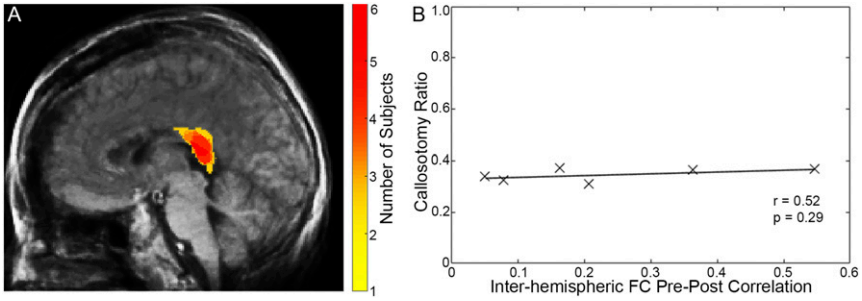

Fig. S1. Residual CC after partial callosotomy. (*A*) An overlap analysis of the posterior portion of the CC that was spared by the partial callosotomy procedure. The heat map identifies the number of subjects where overlap occurs for each voxel at $x = -4$. The size and shape of an individual's CC is variable, but the sparing of the splenium was consistent in the partial callosotomy procedure. (*B*) The proportion of callosum sectioned (posterior third including the splenium) was consistent across partial subjects and did not show a significant association with similarity of interhemispheric FC precallosotomy and postcallosotomy.

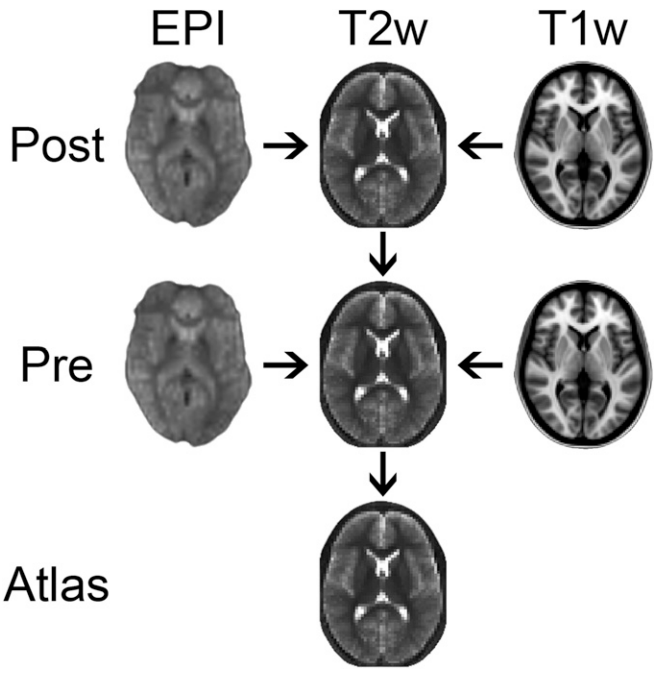

Fig. S2. Image alignment procedure. Precallosotomy T2w images were registered to a T2w atlas representative target. Then postcallosotomy T2w was aligned to the precallosotomy T2w. T1w and EPI images were aligned to the respective T2w image by cross-modal registration.

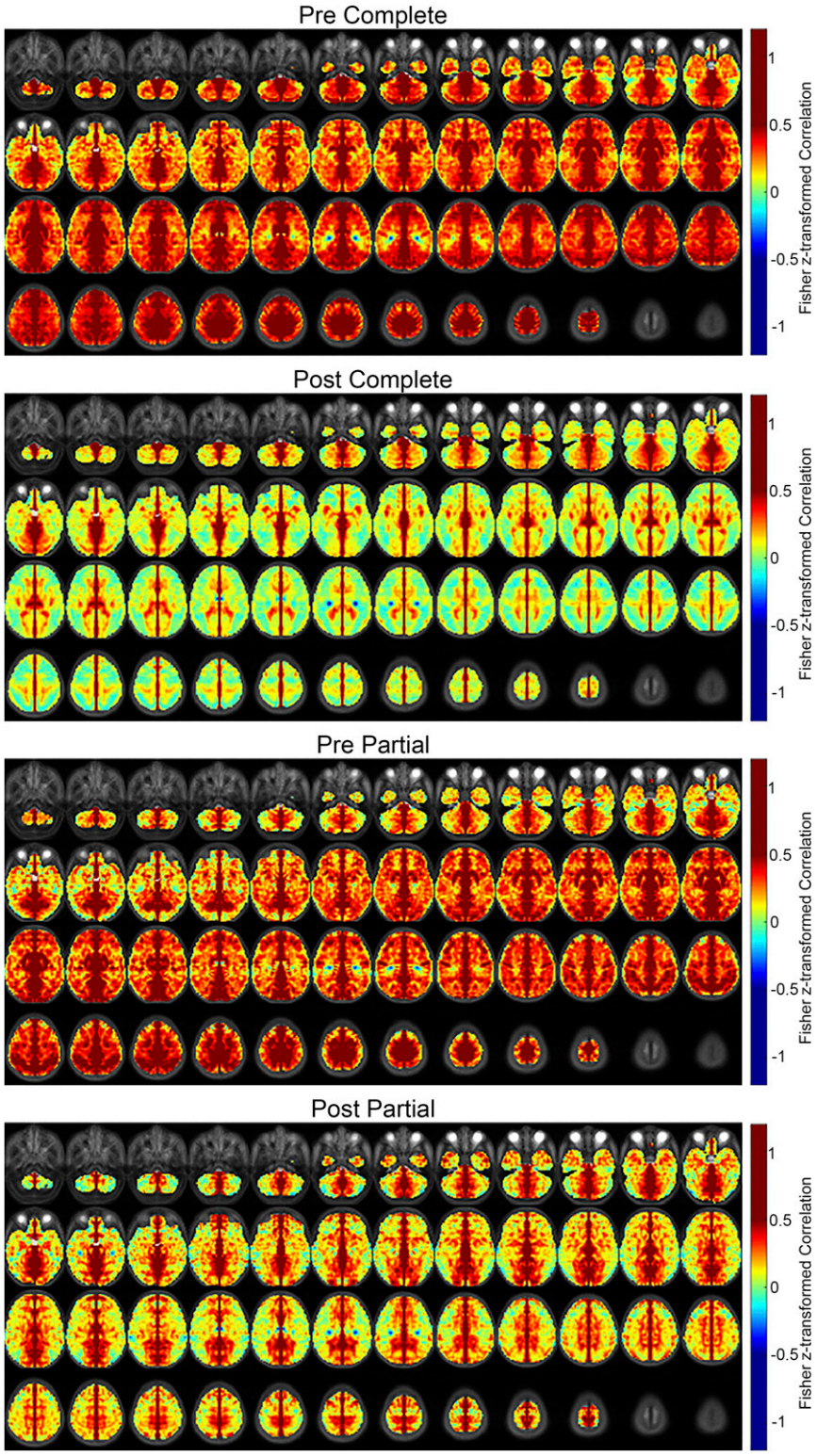

Fig. S3. Full VMHC maps. Mean VMHC maps for all slices are displayed in a similar format to the exemplar images in Fig. 4*A*.

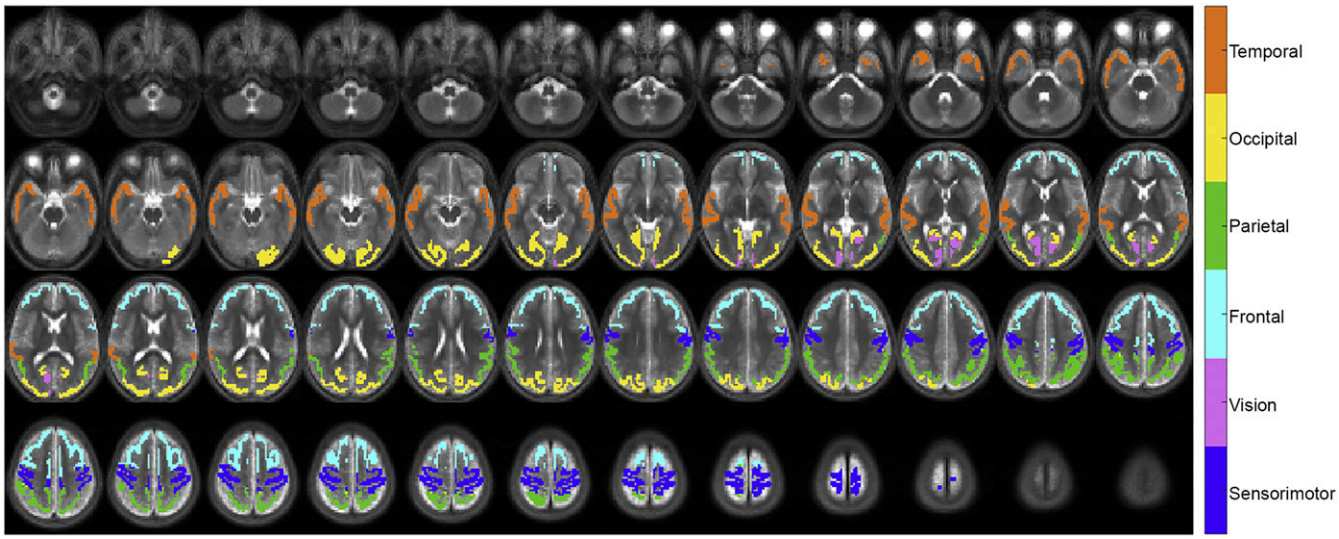

Fig. S4. Anatomic labels by Brodmann area. The anatomic labels used for sampling VMHC precallosotomy and postcallosotomy are overlaid on the T2w atlas representative image. Anatomic labels include primary sensorimotor (blue), primary vision (purple), frontal (cyan), parietal (green), occipital (yellow), and temporal (orange) cortical areas.

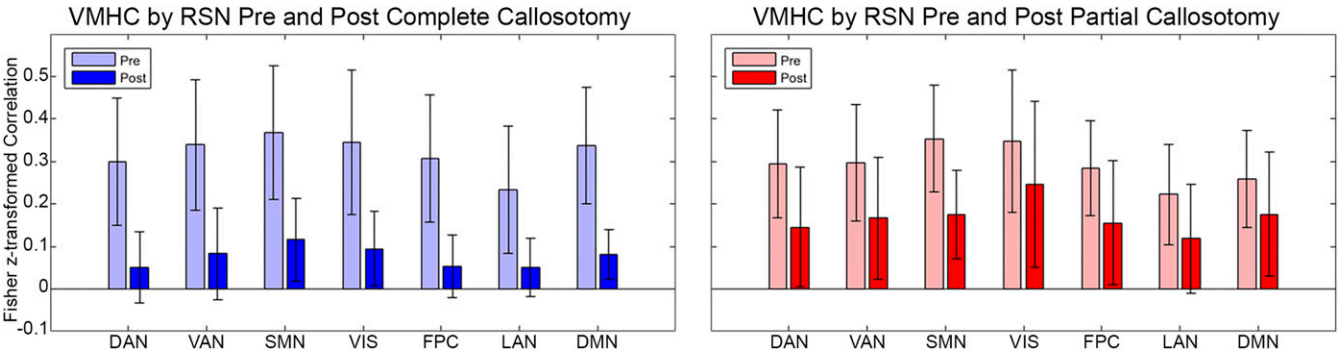

Fig. S5. Change in VMHC by RSN. Mean (and 95% confidence interval) VMHC precallosotomy and postcallosotomy by RSN are displayed in bar graph format for complete and partial callosotomy. Voxels were assigned to one of seven RSNs including DAN, DMN, FPC, LAN, SMN, VAN, and VIS. Membership to each RSN was determined by a previously published group average winner-take-all map (Fig. S6).

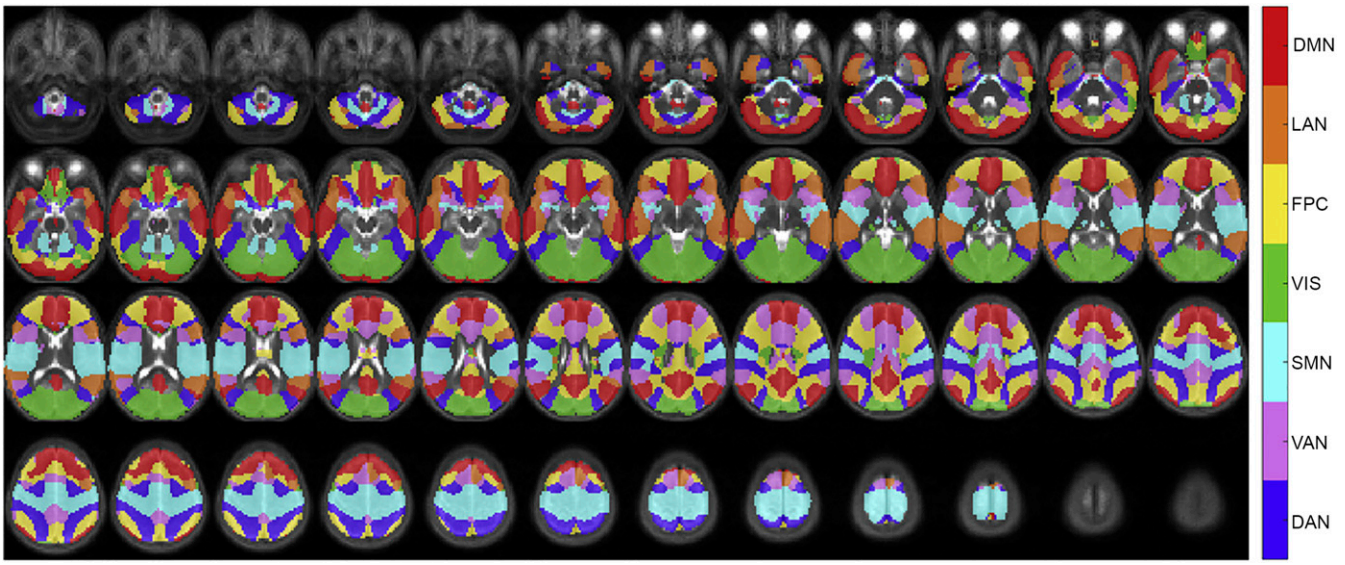

Fig. S6. RSN labels. The RSN labels used for sampling VMHC precallosotomy and postcallosotomy overlaid on the T2w atlas representative image. RSN labels include DAN, blue; DMN, red; FPC, yellow; LAN, orange; SMN, cyan; VAN, purple; VIS, green.

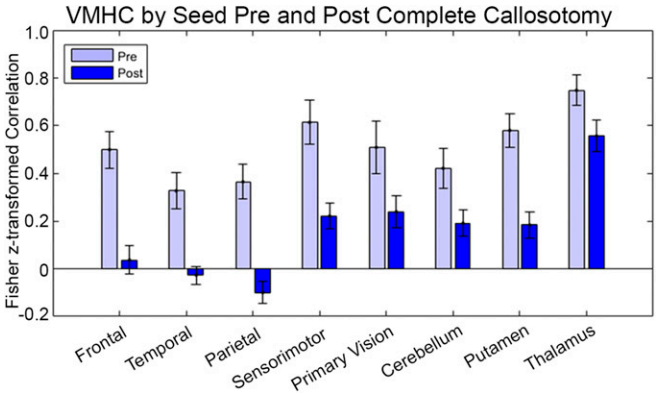

Fig. S7. Change in VMHC including regions not disconnected. VMHC is examined by placing a seed in select regions before and after complete callosotomy. The cerebellum, putamen, and thalamus represent regions without direct connections via the CC. The cerebellum and putamen show similar degree of decrease in VMHC compared with sensorimotor and primary vision areas but less so than more associative cortical areas such as the frontal, temporal, and parietal areas. The thalamus showed the least change after complete callosotomy. Error bars represent 95% confidence intervals.

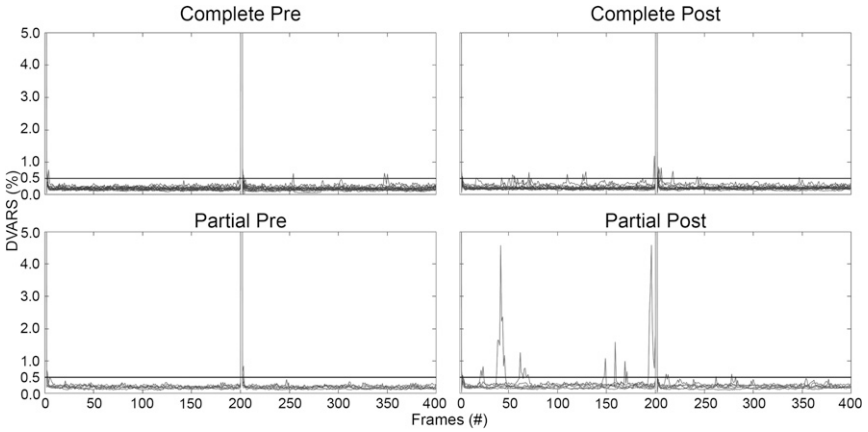

Fig. S8. DVARS movement data. The DVARS are plotted for all subjects by complete and partial groups precallosotomy and postcallosotomy. The horizontal bold line marks the 0.5% DVARS threshold at which frames where censored for motion. Four hundred frames total were collected in two runs of 200 frames each for all sessions. Very little movement is noted across all subjects owing to the effect of sedation used for both sessions.

Table S1. Subject characteristics

Subject	Callosotomy	Age, y	Sex	Sedation preprocedure	Sedation postprocedure	Antiepileptic drugs
1	Partial	2.3	F	Propofol	Propofol	Levetiracetam, Rufinamide/Banzel, Clobazam
2	Complete	3.2	M	Propofol	Dexmedetomidine	Clobazam, Felbamate, Valproic acid
3	Complete	4.9	F	Propofol	Propofol	Felbamate, Phenobarbital
4	Complete	5.1	M	Propofol	Pentobarbitol	Clobazam, Phenobarbital
5	Partial	5.5	M	Propofol	Dexmedetomidine	Zonisamide, Carbamazepine
6	Complete	6.1	M	Propofol	Propofol	Levetiracetam, Lamotrigine, Ethosuximide
7	Complete	7.6	F	Propofol	Propofol	Felbamate
8	Complete	7.8	M	Propofol	Propofol	Lamotrigine, Methsuximide
9	Complete	7.9	F	Propofol	Remifentanil	Felbamate, Topiramate, Valproic acid
10	Partial	9.3	M	Propofol	Propofol	Felbamate, Topiramate, Clobazam
11	Complete	10.7	F	Propofol	Propofol	Clonazepam, Felbamate
12	Complete	11.7	M	Propofol	Pentobarbitol	Clobazam, Felbamate, Levetiracetam, Zonisamide
13	Complete	12.1	M	Propofol	Ativan	Lacosamide, Levetiracetam, Zonisamide
14	Partial	12.1	M	Propofol	Propofol	Valproate, Felbamate, Clonazepam, Methsuximide
15	Complete	12.4	M	Propofol	Propofol	Lamotrigine, Levetiracetam, Valproic acid
16	Partial	12.5	M	Propofol	Propofol	Levetiracetam, Felbamate, Rufinamide
17	Complete	12.8	M	Propofol	Propofol	Citalopram, Rufinamide, Topiramate
18	Partial	13.4	M	Propofol	Propofol	Clonazepam, Levocarnitine
19	Complete	13.4	M	Propofol	Pentobarbitol	Felbamate, Lamotrigine, Topiramate
20	Complete	15.1	M	Propofol	Dexmedetomidine	Clobazam, Felbamate, Valproic acid
21	Complete	15.6	F	Propofol	Propofol	Felbamate, Topiramate, Valproic Acid
22	Complete	17.2	M	Propofol	Propofol	Clobazam, Lacosamide

F, female; M, male.